RSC Advances

PAPER

View Article Online
View Journal | View Issue

Cite this: *RSC Adv.*, 2021, **11**, 8530

Effects of the addition of CeO_2 on the steam reforming of ethanol using novel carbon-Al_2O_3 and carbon-ZrO_2 composite-supported Co catalysts†

Atsushi Ishihara, * Hiroshi Tsujino and Tadanori Hashimoto

Received 7th January 2021
Accepted 5th February 2021

DOI: 10.1039/d1ra00141h

rsc.li/rsc-advances

Novel carbon-Al_2O_3 and carbon-ZrO_2 composite-supported Co catalysts were prepared using the sol–gel method with polyethylene glycol (PEG) as a carbon source, and the effects of the addition of CeO_2 to catalysts on the steam reforming of ethanol were investigated. The reactions were carried out in a fixed bed reactor with H_2O/EtOH = 12 (mol/mol) and a temperature range of 300 °C to 600 °C. The catalyst characterization was performed by XRD, nitrogen adsorption and desorption isotherms, TG-DTA, XRF and TEM. Although the carbon-Al_2O_3 composite-supported Co catalysts exhibited a higher conversion of ethanol than the carbon-ZrO_2 composite-supported Co catalysts, the effect of the addition of CeO_2 was hardly observed for catalysts with Al_2O_3. In contrast to the case of catalysts with Al_2O_3, the effect of the addition of CeO_2 to catalysts with ZrO_2 on the conversion and the hydrogen yield was observed, and the hydrogen yield at 600 °C exceeded that of catalysts with Al_2O_3. 16Co42C31.5Ce10.5Zr exhibited the highest hydrogen yield of 89% at 600 °C. Fine Co metal species were observed for the used ZrO_2-based catalysts, while Co_3O_4 peaks were observed for the used Al_2O_3-based catalysts. The development of the carbon nanotube-like structure with a diameter of 50 nm was observed with particles having diameters of 30 nm to 50 nm, suggesting that the carbon deposition might occur so as not to deactivate the catalyst.

1. Introduction

Restrictions on the utilization of fossil fuels have begun in developed countries of Europe and have spread throughout the world. In such situations, the technology for the utilization of renewable energy has to be developed urgently and the reforming of biomass has been one of the candidates.[1] Among such renewable resources, is ethanol obtained from fruits and grains, and much attention has been focused on its steam reforming.[1,2] While ethanol may be directly utilized for fuel, the production of hydrogen from ethanol has been one of the most attractive technologies. The steam reforming of methane is carried out using supported Ni-based catalysts. However, it is known in the steam reforming of ethanol (SRE) that the selectivity for hydrogen of Ni catalysts is not so high as that for Co-based catalysts.[1,2] Co catalysts supported on alumina were reported for their high hydrogen yield although they were often deactivated by coke deposition. In these reports, it was suggested that Co metal supported on an oxide would be an active site for SRE.[1–17] The promotion effects of Pt, Pd, Ru, and Ir were observed in SRE using Co/Al_2O_3, and among them, the addition of Ru was the most effective.[10] Co and Ni catalysts supported on perovskite were also active for SRE.[11] The addition of Fe to Co/α-Al_2O_3 promoted SRE.[14] The addition of Ni and Co to Cu/ZnO/Al_2O_3 also promoted SRE.[15] The performance of Co/SiO_2 for SRE was higher than that of Co/Al_2O_3 since Co was not sufficiently reduced on Co/Al_2O_3 due to the presence of the strong interaction between Al_2O_3 and Co species.[16] The effect of the addition of Co species to Ni/Al_2O_3 was confirmed in oxidative SRE where Ni and Co oxides on alumina were reduced at the lower temperature and led to more stable activity and yield of hydrogen.[17] As other catalysts, Co/ZnO–Al_2O_3,[18] Co/CeO_2,[19–21] Co/ZrO_2,[19,21] Rh/Co/CeO_2 or Al_2O_3,[22] K/Co/Al_2O_3,[23,24] Co/CaO–Al_2O_3,[25] Cu promoted Ni–Co/hydrotalcite[26] for SRE, Co/Al_2O_3 and Co/$CeO_2Al_2O_3$ for oxidative SRE,[27] and Co–CaO/CeO_2, ZrO_2 and MgO,[28] CaO–Ni/Al_2O_3 (ref. 29) for sorption enhanced SRE have been reported to have superior activity and selectivity. Further, it has been reported that CeO_2–ZrO_2 composite-supported cobalt and rhodium catalysts have higher activity and selectivity in SRE.[20,30–41] For example, when Co(10%)Pt(3%)/CeO_2–ZrO_2–Al_2O_3 was used with a Pd membrane, 60% conversion and 70% hydrogen recovery were achieved at 400 °C.[30] RhPd/$Ce_{0.5}Zr_{0.5}O_2$–Al_2O_3 exhibited high performance and stability in SRE.[31] When the CeO_2–ZrO_2 composite-supported Co, Ni and NiCo catalysts were compared in SRE, the NiCo catalyst exhibited superior performance, while the Co catalyst was not so active.[32] When Co, Fe and Rh were added to Ni/CeO_2–ZrO_2 catalysts, NiRh/CeO_2–ZrO_2 exhibited good performance for 400 h in SRE.[33] Bimetallic CoIr/$Ce_{1-x}Zr_xO_2$ catalysts were also

Division of Chemistry for Materials, Graduate School of Engineering, Mie University, Mie, Japan. E-mail: ishihara@chem.mie-u.ac.jp

† Electronic supplementary information (ESI) available. See DOI: 10.1039/d1ra00141h

used in the oxidative steam reforming of a bio-butanol raw mixture and the catalyst with the better performance was found to inhibit the sintering of active metal and the coke formation.[34,35] It has been found that 10%Co/CeO_2–ZrO_2 exhibited 80% of hydrogen yield and 100% of ethanol conversion for ethanol steam reforming at 450 °C with a steam-to-carbon ratio of 6.5.[38,39] Also, 10%Co/10%CeO_2–ZrO_2 exhibited about 75% of stable hydrogen yield and 100% of ethanol conversion at 450 °C with the molar ratio of EtOH : H_2O = 1 : 10.[40] A catalyst with 9.1 wt% Co and 22.3 wt% Ce supported on nanopowder ZrO_2 exhibited the conversion of ethanol 100%, 92% H_2, 81% CO_2, 6% CO and 12% CH_4 in SRE with H_2O/EtOH = 21 mol/mol at 420 °C.[41] In these studies, the conversion of ethanol reached 100% at a temperature near 450 °C, while the hydrogen yield has not yet been determined and there have been differences in results between research groups. Further, the effects of the combination and its ratio of CeO_2 and other oxides, and the role of CeO_2 in these catalyst systems have not yet been sufficiently understood.

Although supported Co catalysts exhibited high activity in SRE, active species may be metallic cobalt or cobalt oxides, and arguments remain. It seems that oxide-supported cobalt species would be reduced to the metallic state and that the successive interaction with oxide support may stabilize metallic species, which would lead to a decrease in the activity. In contrast, some metal oxides may generate both metal and oxide species in an interface, where metal species may have high dispersion and bring about high activity.

Our group has already reported that Fe and Co catalysts supported on carbon-oxide composites were active for the Fischer–Tropsch reaction in the presence of solvent[42] and Ni catalysts were effective for the hydrothermal gasification of phenol dissolved in water.[43–45] In the reports, metallic species were maintained on carbon-coated oxide supports, which inhibited the interaction between oxides and metal species and increased the activity. Further, we have found that the carbon-oxide composite-supported Ni and Co catalysts were active for the SRE reaction. The Ni/C/Al_2O_3 catalyst showed high activity and the Co/C/Al_2O_3 catalyst exhibited a high hydrogen yield for SRE. In the present study, we tried to test catalysts consisting of not only Co/C/Al_2O_3 but also Co/C/ZrO_2 in SRE and the effects of the addition of CeO_2 to both catalyst systems on SRE were investigated. Only the ZrO_2-based catalyst system exhibited the effects of the addition of CeO_2 and that CeO_2-modified ZrO_2-based catalysts exhibited a higher yield of hydrogen as compared to Al_2O_3-based catalysts.

2. Experimental

2.1. Preparation of carbon-Al_2O_3 and ZrO_2 composite-supported Co catalysts with and without CeO_2

Starting materials for Al_2O_3 and ZrO_2 were aluminum tri-*sec*-butoxide (ASB, $C_{12}H_{27}Al_2O_3$, Tokyo Kasei) and zirconium(IV) butoxide (ZB, $(C_4H_9O)_4Zr$, *ca.* 80% in 1-butanol, Tokyo Kasei). CeO_2 was a reference catalyst from the Catalysis Society of Japan, JRC-CEO-3. A carbon source was polyethylene glycol (PEG, $(CH_2–CH_2–O)_n$, Nakalai Tesque). A cobalt source was cobalt nitrate hexahydrate ($Co(NO_3)_2 \cdot 6H_2O$, Nakalai Tesque). The catalyst was prepared using the sol–gel method according to the flowchart shown in Fig. S1.†

For an example, 16Co42C21Ce21Zr 700N_2 was prepared as follows: a 1-butanol solution of ZB (4.09 g ZB, 15.16 g 1-butanol) in a 200 mL beaker was mixed with ceria (0.53 g). To the mixture, a 1-butanol solution of cobalt nitrate (3.95 g cobalt nitrate hexahydrate, 9.29 g 1-butanol) was added dropwise at 0 °C. Further, 3.89 g of PEG was added and then the mixture was stirred at 0 °C for 10 h. The mixture was dried at 115 °C for 8 h and the gel obtained was pushed out of a syringe for ceramics to make cylindrical pellets with a diameter of 3 mm. The pellets were calcined under nitrogen atmosphere at 700 °C for 3 h to prepare catalysts that were crushed to particles with sizes 125–355 and 355–600 μm, in a weight ratio of 7 : 3. 16Co63C21A, 16Co42C21Ce21A, 16Co63C21Zr, 16Co42C10.5Ce31.5Zr and 16Co42C31.5Ce10.5Zr were prepared using a similar method.

Sample names were expressed as follows: Co was cobalt, C was carbon from PEG, Ce was ceria, Zr was zirconia, A was alumina and figures before abbreviations represent values of wt%. For example, 16Co42C21Ce21Zr is a catalyst having Co metal of 16 wt%, C of 42 wt%, CeO_2 of 21 wt% and ZrO_2 of 21 wt%.

2.2. Steam reforming of ethanol using carbon-Al_2O_3 and ZrO_2 composite-supported Co catalysts with and without CeO_2

Fig. S2† shows an apparatus for the SRE reaction. A fixed bed flow reactor of stainless steel (ID 8 mm) and a back pressure regulator were used. Here, 1 g catalyst was added in the order, quartz sand, glass wool, catalyst, glass wool and quartz sand from the top to the bottom in the center of the reactor. The condition of the steam reforming was as follows: the reaction temperature was in the range of 300–600 °C, the heating rate was 5 °C min^{-1}, LHSV was 48 h^{-1}, the volume of a catalyst was 0.5 mL and H_2O/EtOH was 12 mol/mol. The pressure in the inlet of the reactor changed depending on the catalysts used and the temperature, and increased with the progress of the reaction. The pressure for each catalyst at 600 °C is tabulated in Table 1 and all data are tabulated in Table S1.† The reaction temperature was kept at each tested temperature for 1 h and then products were collected every 30 min for 1 h, that is, two times. The obtained products were separated in the gas–liquid separator. Gaseous products collected in a Tedlar bag were determined using a gas chromatograph with a thermal conductivity detector (GC-TCD, Shimadzu GC-8A). Liquid products were determined using a gas chromatograph with a flame ionization detector (GC-FID, Shimadzu GC-2014) to obtain the ethanol conversion.

A liquid product (1 μL) injected into GC-FID by the auto-sampler (AOC-20i) was determined under the following conditions: injection temperature 250 °C, detector temperature 250 °C, initial column temperature 50 °C for 3 min, final column temperature 200 °C, pressure 107.8 kPa, flow rate of N_2 carrier gas 153.7 mL min^{-1}, sprit ratio 200, BP-1 column with a length 60 m, column diameter 0.25 mm and film thickness 0.5 μm. H_2 was determined using GC-TCD under the conditions of nitrogen carrier gas, gaseous product sample 0.1 mL, injection temperature 110 °C, detector temperature 110 °C, column temperature 50 °C, column length of 2 m and column Porapak T. Carbon monoxide, carbon dioxide and methane were determined using GC-TCD under the conditions of He carrier gas,

Table 1 EtOH conversion, H_2 yield, carbon gas selectivity and inlet pressure in the steam reforming of ethanol at 600 °C[a]

Sample name	EtOH conv. (%)	H_2 yield (%)	CO selct. (%)	CO_2 selct. (%)	CH_4 selct. (%)	Total C gas (%)	Inlet pressure (MPa)
16Co63C21Al	100	80	12	71	17	100	0.39
16Co42C21Ce21Al	100	76	11	59	12	82	0.15
16Co63C21Zr	99	63	8	39	15	62	1.86
16Co42C10.5Ce31.5Zr	96	61	9	52	11	72	0.68
16Co42C21Ce21Zr	100	84	20	46	10	76	0.14
16Co42C31.5Ce10.5Zr	100	89	9	73	18	100	0.42

[a] Conv. = conversion; selct. = selectivity; C gas = CO, CO_2 and CH_4.

gaseous product sample 0.1 mL, injection temp. of 110 °C, detector temp. of 110 °C, column temp. of 150 °C and a packed column of Unibeads C with column length of 3 m.

2.3. Characterization of carbon-Al_2O_3, ZrO_2 and CeO_2 composite-supported Co catalysts

A Rigaku Ultima IV was used to obtain X-ray diffraction (XRD) patterns of crystals of the catalyst, which were measured under the conditions of Ni-filtered Cu-Kα radiation ($\lambda = 0.15418$ nm), 0.10 g catalyst on a plate of slide glass, 2θ in the range 10° to 70°, continuous scan, sampling width 0.01°, scan speed 4° min^{-1}, radiation slit 1/3°, radiation column limitation slit 10.00 nm, scattering slit 1/3°, detecting slit 0.30 nm, offset angle 0°, voltage 40 kV and current 40 mA.

Nitrogen adsorption and desorption were performed using a BELSORP-mini I-MSP to estimate pore volumes, surface areas and pore diameters by BET and BJH methods. TG-DTA using DTG-60AH (Shimadzu) was measured under the following conditions: temperature from 25 °C to 800 °C, heating rate of 10 °C min^{-1}, catalysts of 10 mg, a platinum pan, and an air atmosphere to estimate the content of carbonaceous materials in fresh and used catalysts. XRF using EDX-720 (Shimadzu) was measured to estimate the content of inorganic matter in the catalyst. TEM images were obtained using JEM-1011 (Nihon Denshi, BEAM current: 60 μA).

3. Results and discussion

3.1. Ethanol steam reforming using carbon-Al_2O_3, ZrO_2 and CeO_2 composite-supported Co catalysts

Fig. 1 and 2 show the effect of temperature on the conversion of ethanol and the yield of hydrogen in the steam reforming of ethanol using carbon-Al_2O_3–CeO_2 and carbon-ZrO_2–CeO_2 composite-supported Co catalysts, respectively. Table 1 summarizes ethanol conversions, hydrogen yields, carbon recoveries of CO, CO_2 and CH_4 against converted ethanol and the inlet pressure at the reaction temperature of 600 °C. Carbon-Al_2O_3 composite-supported Co catalysts exhibited higher conversions than carbon-ZrO_2 composite-supported Co catalysts and the conversion reached 100% at 500 °C, while the addition of CeO_2 hardly affected the conversions for the catalysts with Al_2O_3. In contrast, the effect of the addition of CeO_2 was observed for catalysts with ZrO_2 and the conversions changed depending on the amounts of ZrO_2 and CeO_2 added. As shown in Fig. 2a, the yields of hydrogen for 16Co63C21Al and 16Co42C21Ce21Al increased with increasing temperature and reached 80% and 76% at 600 °C, respectively, indicating that there was no positive effect resulting from the addition of CeO_2. In contrast, the yields of hydrogen for 16Co63C21Zr, 16Co42C10.5Ce31.5Zr, 16Co42C21Ce21Zr and 16Co42C31.5-Ce10.5Zr at 600 °C were 63%, 61%, 84% and 89%, respectively, indicating that catalysts with larger amounts of CeO_2 exhibited higher hydrogen yields, which were higher than those for catalysts with Al_2O_3. The carbon recoveries of 16Co42C31.5Ce10.5Zr and 16Co63C21Al catalysts reached 100% at 600 °C. The selectivities of CO, CO_2 and CH_4 for 16Co42C31.5Ce10.5Zr were 9, 73 and 18%, respectively, and were very similar to those for 16Co63C21Al. As the carbon recoveries for other catalysts were lower than those for 16Co42C31.5Ce10.5Zr and 16Co63C21Al, it seems that significant carbon deposition would have occurred. The result was confirmed by the high value of the pressure in the reactor inlet at 600 °C as given in Table 1 and the fact that the carbon content of the catalyst after the reaction was higher than that before the reaction as shown in Table 2.

As reported in the literature,[28] when recycling was repeated, deactivation was observed. Although the recycling experiments are not reported in the present study, the change in the inlet

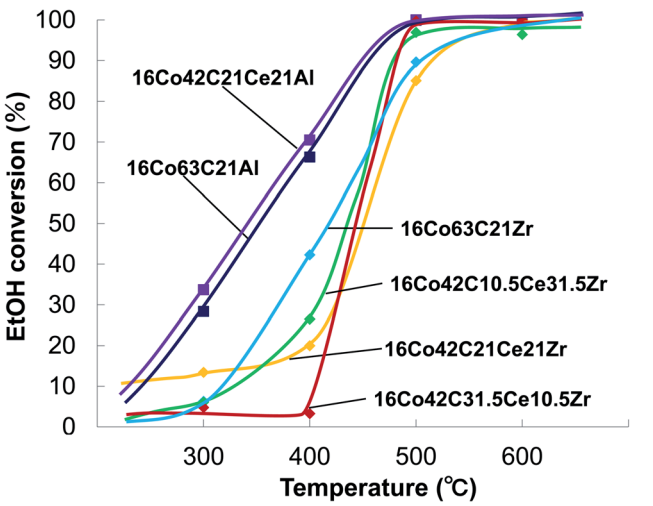

Fig. 1 The effect of temperature on EtOH conversion in the steam reforming of ethanol.

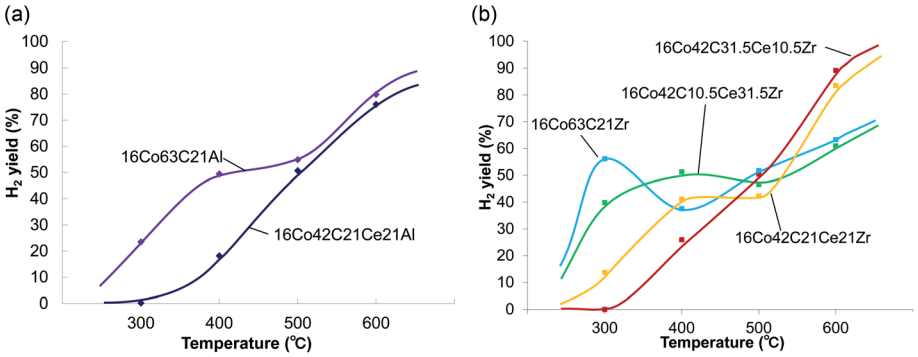

Fig. 2 The effect of temperature on H_2 yield in the steam reforming of ethanol using (a) carbon-alumina composite-supported cobalt catalysts and (b) carbon-zirconia composite-supported cobalt catalysts.

pressure with increasing temperature as shown in Table S1† could be referred to in order to predict the reactivity for this type of catalyst. At 300 and 400 °C, the pressure was rather low for each catalyst because of the low activity. At 500 °C, the pressure increased rapidly because the steam reforming started but the formation of coke and less reactive intermediates would be faster than CO and CO_2 formation. However, at 600 °C the pressure decreased in some catalysts because the oxygen from water started to act for the removal of coke and less reactive intermediates and the formation of CO and CO_2 on the catalysts. The results suggested that the coke and the less reactive intermediate could be removed by the appropriate oxidation to disperse metal species again and the reduction to obtain a clean metal surface on a catalyst.

According to the previous reports of SRE catalyzed by Co/CeO_2–ZeO_2, the effect of the feed concentration on the activity and the hydrogen yield would be rather low and the H_2 formation reaction seems to proceed rapidly after the C–C bond scission of ethanol.[38,39]

Table 2 Elemental analysis for carbon-oxide composite-supported metal catalysts by XRF and TG-DTA[a]

	Weight ratio (wt%)			
Al catalyst	Co	C	CeO_2	Al_2O_3
16Co63C21Al*[b]	48.17	17.45	0	34.38
16Co63C21Al*[a]	42.97 (Co_3O_4)	36.46	0	20.57
16Co42C21Ce21Al*[b]	18.5	1.00	43.09	37.76
16Co42C21Ce21Al*[a]	27.10 (Co_3O_4)	33.54	23.19	16.16
	Weight ratio (wt%)			
Zr catalyst	Co	C	CeO_2	ZrO_2
16Co63C21Zr*[b]	32.06	34.93	0	33.01
16Co63C21Zr*[a]	15.97	69.29	0	14.74
16Co42C10.5Ce31.5Zr*[b]	25.44	12.76	14.5	47.65
16Co42C10.5Ce31.5Zr*[a]	10.39	63.24	5.77	20.60
16Co42C21Ce21Zr*[b]	21.70	7.92	28.65	39.48
16Co42C21Ce21Zr*[a]	8.41	67.68	11.86	12.03
16Co42C31.5Ce10.5Zr*[b]	28.11 (Co_3O_4)	0.10	48.36	23.43
16Co42C31.5Ce10.5Zr*[a]	11.5	53.95	23.49	11.40

[a] b: fresh catalyst, a: used catalyst.

3.2. Characterization of carbon-Al_2O_3-ZrO_2-CeO_2 composite-supported Co catalysts

N_2 adsorption and desorption isotherms were determined to estimate the pore structure of the carbon-oxide composite-supported cobalt catalysts and the results are shown in Table 3. Surface areas (SA) were estimated by the BET and BJH methods. Since only mesopores having pore diameters larger than 3.3 nm are estimated by the BJH method, the difference between BET-SA and BJH-SA could likely be derived from the existence of micropores in the estimation of BET-SA. The catalysts with Al_2O_3 included significant amounts of not only mesopores but also micropores. The catalysts with ZrO_2 also included not only mesopores but also micropores, however, the values of surface area were much smaller than those of catalysts with Al_2O_3. The addition of CeO_2 decreased the values of BET-SA for both catalysts with Al_2O_3 and ZrO_2, indicating that CeO_2 would not have micropores. Most of the pore volumes were made up of mesopores and the contribution of micropores to pore volume was small, especially for catalysts with CeO_2. All the catalysts exhibited increases in BET-SA, TPV, BJH-SA, and BJH-PV after the reaction, indicating that significant coke formation would occur and that not only new mesopores but also new micropores could be formed by carbonaceous materials. This was confirmed by the increase of the carbon content in the elemental analysis, which was estimated from the results of TG-DTA and XRF measurements shown in Table 2. Graphite-like signals were also observed in the XRD patterns shown in Fig. 3 and most of the catalysts showed increases in these signals after the reaction. Further, the catalysts with CeO_2 and ZrO_2 exhibited significant development of carbon nanotubes with diameters of 50 nm as shown in the TEM images of Fig. 4.

XRD patterns of carbon-Al_2O_3 composite-supported Co catalysts before reaction are shown in Fig. 3a. Catalysts with Al_2O_3 exhibited Co metal, while signals of Al_2O_3 were not observed in XRD measurement, indicating that Al_2O_3 would also form small particles in the presence of carbon as it was made by the sol–gel method. It has been proposed that the higher yield of hydrogen and conversion would be derived from

Table 3 N_2 adsorption and desorption measurements for carbon-oxide composite-supported metal catalysts[a]

Sample name	BET SA*1 ($m^2\ g^{-1}$)	Total PV*2 ($cm^3\ g^{-1}$)	Avg. PD*3 (nm)	BJHSA*1 ($m^2\ g^{-1}$)	BJHPV*2 ($cm^3\ g^{-1}$)	BJHPD*3 (nm)
16Co63C21Al*b	216	0.32	6.0	96	0.26	3.7
16Co63C21Al*a	238	0.41	7.0	156	0.36	3.7
16Co42C21Ce21Al*b	124	0.29	9.2	83	0.25	10.7
16Co42C21Ce21Al*a	227	0.52	9.2	145	0.48	3.7
16Co63C21Zr*b	120	0.21	6.9	76	0.18	3.7
16Co63C21Zr*a	216	0.58	10.6	139	0.53	3.7
16Co42C10.5Ce31.5Zr*b	91	0.15	6.6	82	0.14	3.7
16Co42C10.5Ce31.5Zr*a	155	0.38	9.7	113	0.35	3.7
16Co42C21Ce21Zr*b	88	0.16	7.5	82	0.16	3.7
16Co42C21Ce21Zr*a	141	0.43	12.2	104	0.41	3.7
16Co42C31.5Ce10.5Zr*b	46	0.15	13.0	55	0.15	9.2
16Co42C31.5Ce10.5Zr*a	131	0.42	12.8	108	0.40	10.6

[a] SA: surface area, PV: pore volume, PD: pore diameter, b: fresh catalyst, a: used catalyst.

the initial reduction of Co species to Co metal in the preparation.[1] With the addition of CeO_2, Co metal was also observed while signals of Al_2O_3 were not observed. As signals of cubic CeO_2 were observed, this indicated that the particle size of Al_2O_3 prepared by the sol–gel method with aluminum alkoxide was much smaller than that of CeO_2. XRD patterns of carbon-ZrO_2 composite-supported Co catalysts before the reaction are also shown in Fig. 3a. In contrast to the Al_2O_3-based catalysts, crystals of tetragonal ZrO_2 as well as Co metal were observed in the catalysts with ZrO_2. It is known that the monoclinic ZrO_2 phase is stable at temperatures of 500 °C and higher,[20,39,46] while the tetragonal ZrO_2 phase also exists in the presence of other metal oxides[34,46] and at the calcination temperature of 400 °C.[33,46] In our present case, there would be such an effect of coexistence. Further, the significant accumulation of crystals of carbon was also observed in 16Co63C21Zr before the reaction, indicating that the crystallization of carbon would proceed on Co metal. With the addition of CeO_2, this development of carbon crystals was inhibited probably because oxygen atoms of PEG would be appropriately provided from CeO_2 to carbon species developed on Co metal. This was also supported by the results from the elemental analysis in Table 2, where 16Co63C21Zr before use included about 34 wt% of carbon although other catalysts with CeO_2 decreased the carbon content by increasing the amount of CeO_2. Co_3O_4 was also observed for 16Co42C31.5Ce10.5Zr, probably because of the high ability of oxygen transfer by a large amount of CeO_2. When CeO_2–ZrO_2 supports were prepared by the coprecipitation method, CeO_2–ZrO_2 mixed oxides were formed, signals of mixed oxides near cubic CeO_2 signals were observed, and single ZrO_2 signals were not observed.[20,32,33,38,39,47] In our present study, ZrO_2 was made by the hydrolysis of zirconium butoxide but signals of ZrO_2 were observed because CeO_2 was directly used and the CeO_2–ZrO_2 mixed oxide was not formed.

XRD patterns of carbon-Al_2O_3 and carbon-ZrO_2 composite-supported Co catalysts after reaction are shown in Fig. 3b. Although the accumulation of carbon may occur on catalysts with Al_2O_3, the development of carbon crystals was inhibited probably because of the presence of the high surface area of Al_2O_3 where amorphous carbon would be accumulated. The presence of CeO_2 does not seem to play a role in providing oxygen to carbon, probably because the interaction between cobalt and CeO_2 may be weak on the Al_2O_3-based catalyst. In contrast to the catalysts with Al_2O_3, ZrO_2-based catalysts exhibited the effects of CeO_2, which provided oxygen from water to carbon and inhibited the significant accumulation of carbon. However, total amounts of carbon for catalysts with ZrO_2 were larger than those of Al_2O_3 as shown in Table 2 and the

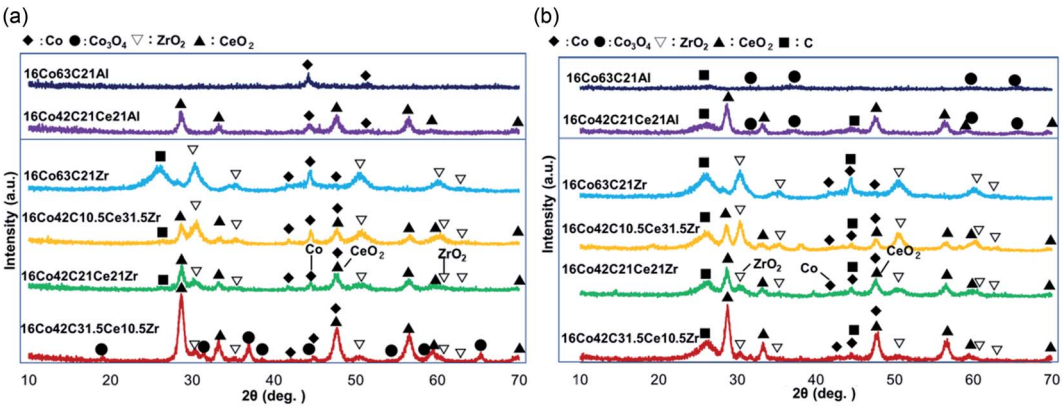

Fig. 3 XRD patterns of carbon-oxide composite-supported cobalt catalysts (a) before use and (b) after use.

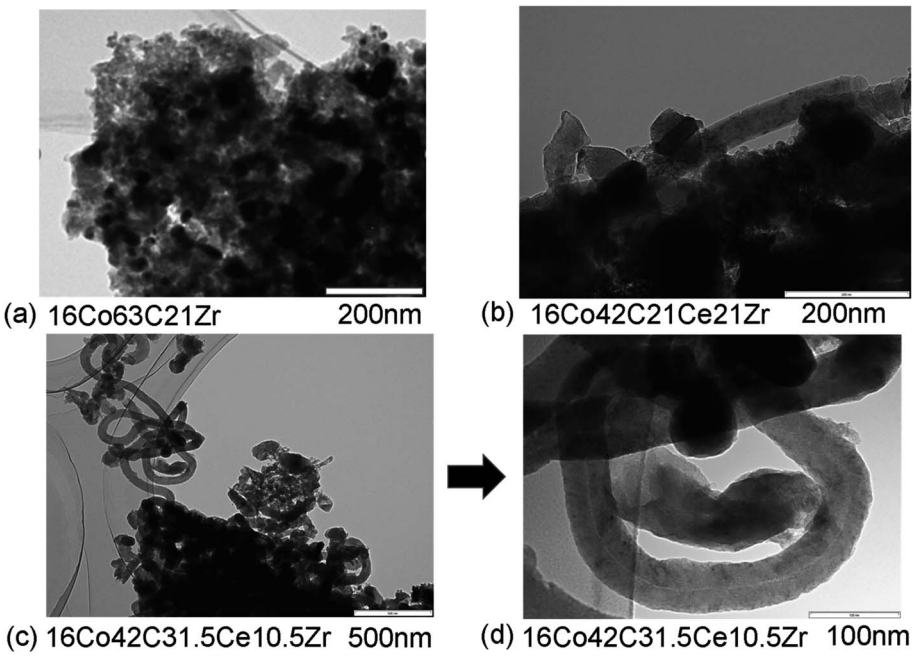

Fig. 4 TEM images of used catalysts, (a) 16Co63C21Zr, (b) 16Co42C21Ce21Zr and (c and d) 16Co42C31.5Ce10.5Zr.

significant development of carbon crystals was observed for catalysts with ZrO_2 probably because of the smaller surface area of ZrO_2-based catalysts. The addition of CeO_2 decreased the development of crystallization of carbon as shown in Fig. 3b, although crystals of carbon somewhat increased for 16Co42C30.5Ce10.5Zr. As the carbon content of 16Co42C30.5-Ce10.5Zr after the reaction shown in Table 2 decreased, the effect of CeO_2 was observed. However, the small surface area of this catalyst may develop the crystallization of carbon species. Signals of Co metal were observed for ZrO_2-based catalysts while Co_3O_4 signals were observed for Al_2O_3-based catalysts. Since both signals of Co metal and Co_3O_4 were very small, it is likely that most of the active Co species that were not detected by XRD would have been dispersed in both catalyst systems.

The elemental analyses of components of catalysts including carbon content were performed by XRF and TG-DTA and the results are shown in Table 2. Calcination under nitrogen atmosphere changed the original composition of metal, carbon and oxide, which appeared for the catalysts since most of the organic parts of PEG were lost through the thermal decomposition. Specifically, the presence of CeO_2 converted the carbon species and the carbon content decreased significantly with increasing the CeO_2 content. For all the catalysts, significant amounts of carbon were accumulated after the reaction and the extent of the carbon accumulation was higher for the ZrO_2-based catalysts than for the Al_2O_3-based catalysts. ZrO_2-based catalysts had smaller surface areas and therefore the dispersion itself of active Co species may be lower than those for Al_2O_3-based catalysts, which led to the lower conversions for ZrO_2-based catalysts and even to the lower recovery of carbon at 600 °C as shown in Table 1. On the other hand, the presence of CeO_2 improved the mobility of oxygen, the carbon recovery for 16Co42C31.5Ce10.5Zr reached 100% and its carbon content after the reaction shown in Table 2 decreased in comparison with those for other ZrO_2-based catalysts.

TEM images of used catalysts, 16Co63C21Zr, 16Co42C21-Ce21Zr and 16Co42C31.5Ce10.5Zr, are shown in Fig. 4. 16Co63C21Zr included large amounts of carbon after the reaction while its shape of carbon did not seem to be carbon nanotubes as shown in Fig. 4a. In contrast to 16Co63C21Zr, catalysts with CeO_2 generated carbon nanotubes with diameter of about 50 nm. The slightly smaller size of the catalyst particles seemed to be located at the end of the carbon nanotubes. Although the carbon deposition might occur in this type of reaction, it is likely that the formation and the development of this type of carbon nanotube would prevent the deactivation of the catalysts and even increase their pore volumes and surface areas as shown in Table 3. It was reported that 16Co63C21Al had metal species with diameters of 10–30 nm surrounded by materials like carbon nanotubes with 100 nm length and 10 nm width.[1] Similar carbon nanotube-like materials were also reported in SRE over the Co/ZrO_2 catalyst although it exhibited deactivation after 24 h at 450 °C.[40] The diameters of the carbon materials changed in the range from 20 nm to 150 nm, depending on the size of the Co particles. When CeO_2 was added,[40] the deactivation was inhibited and the carbon materials were hardly observed after the reaction. Although carbon materials were observed for the Co catalysts with ZrO_2 and CeO_2 in our present study, it seems that carbon materials formed in the reaction under the low temperature would not damage the catalyst. This would also be supported by the fact that the complete material balance in carbon was obtained at 600 °C as shown in Table 1. Further, the inlet pressure at 600 °C was lower than that at 500 °C in several catalysts as shown in Table S1,† suggesting that surplus carbonaceous materials would be removed with the appropriate progress of the reforming

reaction. As the carbon-ZrO_2 composite-supported Co catalyst without CeO_2 (16Co63C21Zr) showed signals of graphitic carbon in XRD before the reaction, the graphitic carbon may exist without CeO_2 and lead to the deactivation. Metal sizes for the ZrO_2-based catalyst would be larger than those for Al_2O_3-based catalysts, which led to the low dispersion of cobalt species and the lower conversion, especially at the lower temperature. However, it seems that with the help of CeO_2 at higher temperatures, the improvement of the oxygen mobility would have brought about an increase in the activity and the yield of hydrogen.

It was assumed from previous reports of Al_2O_3-supported Co catalysts that the presence of large amounts of Co metal would be needed to obtain the high activity and to inhibit the coke formation in the steam reforming of ethanol.[1,48,49] Further, XRD signals of both Co metal for ZrO_2-based and Co_3O_4 for Al_2O_3-based catalysts were very small and these systems exhibited high activity and hydrogen yield at the higher temperature, suggesting that small particles of metallic Co would exist and play the role of a major active species in the catalyst.

$$CH_3CH_2OH \xrightarrow{Co^0} CH_3CHO + H_2 \quad (1)$$

$$CH_3CHO \xrightarrow{Co^0} Co^I(CH_3CO) + Co^I(H) \quad (2)$$

$$Co^I(CH_3CO) \xrightarrow{Co^0} Co^I(CH_3) + Co^0(CO) \quad (3)$$

$$Co^0(CO) \xrightarrow{2Ce^{IV}(O_{0.5})} CO_2 + Co^0 + 2Ce^{III} \quad (4)$$

$$2Ce^{III} + H_2O + 2Co^I(H) \rightarrow 2Co^0 + 2Ce^{IV}(O_{0.5}) + 2H_2 \quad (5)$$

$$Co^I(CH_3) \xrightarrow{3Co^0,\ 2Ce^{IV}(O_{0.5})} Co^0(CO) + 3Co^I(H) + 2Ce^{III} \quad (6)$$

Ideal reaction routes of steam reforming of ethanol catalyzed by a carbon-ZrO_2-CeO_2 composite-supported Co catalyst can be described by eqn (1)–(6) and Fig. 5. Ethanol can be dehydrogenated to acetaldehyde on Co^0 in eqn (1). Further, the oxidative addition of the C–H bond for acetaldehyde may occur to form $Co^I(CH_3CO)$ and $Co^I(H)$ in eqn (2). Also, in eqn (2), two atoms of Co are described expediently while one Co atom may react to give the $Co^{II}(CH_3CO)(H)$ species. C–C bond scission may occur with the help of Co^0 to form $Co^I(CH_3)$ and $Co^0(CO)$ in eqn (3). In eqn (4), an oxygen atom could be given from $2Ce^{IV}(O_{0.5})$ to $Co^0(CO)$ to form carbon dioxide, Co^0 and $2Ce^{III}$. In this equation, an intermediate $Co^{II}O(CO)$ may exist, although it was not drawn.[50] As in eqn (5), H_2O could react on Ce^{III} to give $Ce^{IV}(O_{0.5})$ and H atoms, which would react with $Co^I(H)$ to form H_2 and Co^0. $Co^I(CH_3)$ could react with Co^0 and $Ce^{IV}(O_{0.5})$ to give $Co^0(CO)$, $Co^I(H)$ and Ce^{III}. It seems that Co^0 metal and CeO_2 could be closely supported on ZrO_2 with a small surface area and that this close position of Co and CeO_2 would enable the reactions of eqn (4) and (5) to proceed. When Al_2O_3 was used, the distance between CeO_2 and Co^0 metal would be too far for active species to interact with each other because of the large surface of Al_2O_3. In the case of CeO_2 only as a support, the surface area of CeO_2 may be too small to increase the activity. When CeO_2 with a high surface area was used, a similar high hydrogen yield was reported.[41] Further, when ZrO_2 was used without CeO_2, the initial high activity similar to that of the CeO_2–ZrO_2 system was shown.[40] However, there would be the late transfer of the oxygen of water to carbonyl species to form carbon dioxide. Although the steam reforming of formed

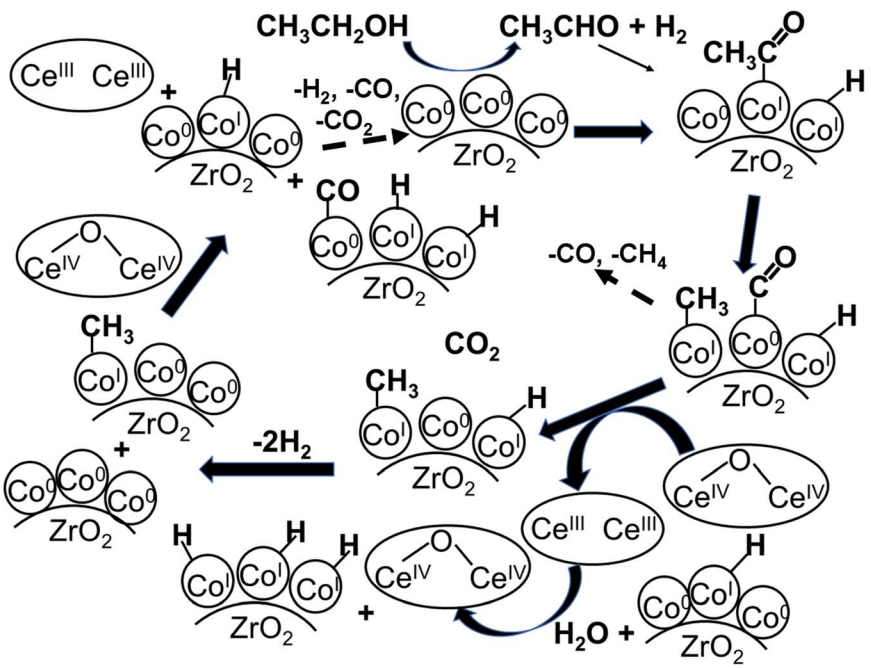

Fig. 5 Ideal reaction routes in the steam reforming of ethanol catalyzed by Co/CeO_2–ZrO_2.

methane at 500 °C and lower than 500 °C was proposed,[21,26,28,31,33,51] it is likely that the methyl group on Co ($Co^{I}(CH_3)$) in eqn (6) would react further before methane formation because methane is difficult to convert once it is formed. The hydrogen transfer from $Co^{I}(CH_3)$ to Co^{0} and the oxygen transfer from $Ce^{IV}(O_{0.5})$ to Co(C) species would produce $Co^{0}(CO)$, $Co^{I}(H)$ and Ce^{III}. When this oxygen transfer is late, carbonaceous species on Co may polymerize, which would lead to coke formation and successive deactivation. It seems that the presence of $Ce^{IV}(O_{0.5})$ next to Co species could properly inhibit the coke formation and the deactivation and that the appropriate use of ZrO_2 support could form such configuration of CeO_2 and Co species. The reaction of $Co^{I}(CH_3)$ with $Co^{I}(H)$ to form methane could always occur with some probability while the configurations of Co and CeO_2 species of such sites for methane formation may be different from those of sites for steam reforming.

It was reported that surface acetate species observed in FT-IR measurements of ethanol TPD could first evolve to monodentate carbonate as an intermediate, then dissociate into CO_2.[40] When water was added to facilitate ethanol conversion, the surface acetate species peaks disappeared at lower temperatures. When FT-IR spectra of adsorbed methanol were measured at temperatures lower than the reaction temperature,[32] methoxy and formate species were observed. Therefore, Fig. S3† was drawn to express the possibility of acetoxylate. This addition of an oxygen atom to surface acetyl species forming an acetoxy group may promote the C–C bond scission and the successive formation of CO_2 and CH_3 species on Co. The ratio of CO and CO_2 formation changed depending on the catalysts used, suggesting that there would be some differences in the mechanism. However, the water gas shift reaction is often proposed to form carbon dioxide in SRE.[28] C–C bond cleavage of acetaldehyde on a metal site was also proposed in SRE.[26,28,33,40] Further, the steam reforming of acetone was stated in SRE.[52] In our experiments, trace amounts of acetaldehyde and acetone were detected at lower temperatures. Therefore, it seems that the mechanism in Fig. 5 is one of the most possible mechanisms.

4. Conclusions

Carbon-Al_2O_3 and ZrO_2 composite-supported Co catalysts were made using the sol–gel method with the addition of PEG as a carbon source. The effects of the addition of CeO_2 to the catalysts on the reactivity in steam reforming of ethanol were investigated in detail. Al_2O_3-based catalysts exhibited higher conversions than ZrO_2-based catalysts, while the effects of the addition of CeO_2 appeared only for ZrO_2-based catalysts. Although the difference in the effects of the combination of CeO_2 and other oxides in SRE catalyzed by supported metal catalysts were not mentioned, the clear superiority of the combination of CeO_2 and ZrO_2 to that of CeO_2 and Al_2O_3 is described in the present study. The conversions of ZrO_2-based catalysts at the lower temperatures decreased with increasing the amounts of CeO_2 added, probably because of their lower surface areas and pore volumes; however, the conversions approached 100% for all the catalysts at 600 °C. Hydrogen yields at 600 °C decreased in the order of 16Co42C31.5Ce10.5Zr > 16Co42C21Ce21Zr > 16Co42C21Ce21Zr = 16Co63C21Zr. Further hydrogen yields for 16Co42C31.5Ce10.5Zr and 16Co42C21Ce21Zr were 89% and 84%, respectively, higher than those for Al_2O_3-based catalysts at 600 °C. ZrO_2-based catalysts accumulated larger amounts of coke, while the accumulation of coke brought about the increase in the surface areas and pore volumes, which would inhibit the deactivation of catalysts. 16Co42C31.5Ce10.5Zr and 16Co42C21Ce21Zr exhibited the formation of carbon nanotubes with diameters of about 50 nm, which would contribute to the increase in the surface areas and pore volumes.

Conflicts of interest

There are no conflicts to declare.

Acknowledgements

The authors thank Mr Yuuta Miki, Mr Akira Andou and Dr Hiroyuki Nasu for their helpful works.

References

1 A. Ishihara, A. Ando, T. Hashimoto and H. Nasu, Steam reforming of ethanol using novel carbon-oxide composite-supported Ni, Co and Fe catalysts, *Fuel Process. Technol.*, 2020, **197**, 106203.
2 P. Riani, G. Garbarino, F. Canepa and G. Busca, Cobalt nanoparticles mechanically deposited on α-Al_2O_3: a competitive catalyst for the production of hydrogen through ethanol steam reforming", *J. Chem. Technol. Biotechnol.*, 2019, **94**, 538–546, DOI: 10.1002/jctb.5800.
3 F. Haga, T. Nakajima, H. Miya and S. Mishima, Catalytic properties of supported cobalt catalysts for steam reforming of ethanol, *Catal. Lett.*, 1997, **48**(3/4), 223–227.
4 S. Cavallaro, N. Mondello and S. Freni, Hydrogen produced from ethanol for internal reforming molten carbonate fuel cell, *J. Power Sources*, 2001, **102**(1–2), 198–204, DOI: 10.1016/S0378-7753(01)00800-X.
5 J. Llorca, N. Homs, J. Sales and P. Ramirez de la Piscina, Efficient Production of Hydrogen over Supported Cobalt Catalysts from Ethanol Steam Reforming, *J. Catal.*, 2002, **209**(2), 306–317, DOI: 10.1006/jcat.2002.3643.
6 A. Kaddouri and C. Mazzocchia, A study of the influence of the synthesis conditions upon the catalytic properties of Co/SiO_2 or Co/Al_2O_3 catalysts used for ethanol steam reforming, *Catal. Commun.*, 2004, **5**(6), 339–345, DOI: 10.1016/j.catcom.2004.03.008.
7 S. Duan and S. Senkan, Catalytic Conversion of Ethanol to Hydrogen Using Combinatorial Methods, *Ind. Eng. Chem. Res.*, 2005, **44**(16), 6381–6386, DOI: 10.1021/ie049202k.
8 H. Song, L. Zhang, R. B. Watson, D. Braden and U. S. Ozkan, Investigation of bio-ethanol steam reforming over cobalt-based catalysts, *Catal. Today*, 2007, **129**(3–4), 346–354, DOI: 10.1016/j.cattod.2006.11.028.

9 D. R. Sahoo, S. Vajpai, S. Patel and K. K. Pant, Kinetic modeling of steam reforming of ethanol for the production of hydrogen over Co/Al_2O_3 catalyst, *Chem. Eng. J.*, 2007, **125**(3), 139–147, DOI: 10.1016/j.cej.2006.08.011.

10 L. P. R. Profeti, E. A. Ticianelli and E. M. Assaf, Production of hydrogen by ethanol steam reforming on Co/Al_2O_3 catalysts: Effect of addition of small quantities of noble metals, *J. Power Sources*, 2008, **175**(1), 482–489, DOI: 10.1016/j.jpowsour.2007.09.050.

11 K. Urasaki, K. Tokunaga, Y. Sekine, M. Matsukata and E. Kikuchi, Production of hydrogen by steam reforming of ethanol over cobalt and nickel catalysts supported on perovskite-type oxides, *Catal. Commun.*, 2008, **9**(5), 600–604, DOI: 10.1016/j.catcom.2007.04.007.

12 A. E. Galetti, M. F. Gomez, L. A. Arrua, A. J. Marchi and M. C. Abello, Study of CuCoZnAl oxide as catalyst for the hydrogen production from ethanol reforming, *Catal. Commun.*, 2008, **9**(6), 1201–1208, DOI: 10.1016/j.catcom.2007.11.015.

13 P. Bichon, G. Haugom, H. J. Venvik, A. Holmen and E. A. Blekkan, Steam Reforming of Ethanol Over Supported Co and Ni Catalysts, *Top. Catal.*, 2008, **49**(1–2), 38–45, DOI: 10.1007/s11244-008-9061-8.

14 Y. Sekine, Y. Nakazawa, K. Oyama, T. Shimizu and S. Ogo, Effect of small amount of Fe addition on ethanol steam reforming over Co/Al_2O_3 catalyst, *Appl. Catal., A*, 2014, **472**, 113–122, DOI: 10.1016/j.apcata.2013.11.026.

15 B. Lorenzut, T. Montini, L. De Rogatis, P. Canton, A. Benedetti and P. Fornasiero, Hydrogen production through alcohol steam reforming on Cu/ZnO-based catalysts, *Appl. Catal., B*, 2011, **101**(3–4), 397–408, DOI: 10.1016/j.apcatb.2010.10.009.

16 A. F. Lucredio, J. D. A. Bellido, A. Zawadzki and E. M. Assaf, Co catalysts supported on SiO_2 and γ-Al_2O_3 applied to ethanol steam reforming: Effect of the solvent used in the catalyst preparation method, *Fuel*, 2011, **90**(4), 1424–1430, DOI: 10.1016/j.fuel.2010.12.036.

17 S. Andonova, C. N. de Avila, K. Arishtirova, J. M. C. Bueno and S. Damyanova, Structure and redox properties of Co promoted Ni/Al_2O_3 catalysts for oxidative steam reforming of ethanol, *Appl. Catal., B*, 2011, **105**(3–4), 346–360, DOI: 10.1016/j.apcatb.2011.04.029.

18 B. Banach and A. Machocki, Effect of potassium addition on a long term performance of Co-ZnO-Al_2O_3 catalysts in the low-temperature steam reforming of ethanol: Co-precipitation vs citrate method of catalysts synthesis, *Appl. Catal., A*, 2015, **505**, 173–182, DOI: 10.1016/j.apcata.2015.08.003.

19 H. Song, L. Zhang and U. S. Ozkan, The Effect of Surface Acidic and Basic Properties on the Performance of Cobalt-Based Catalysts for Ethanol Steam Reforming, *Top. Catal.*, 2012, **55**(19–20), 1324–1331, DOI: 10.1007/s11244-012-9918-8.

20 P. Rybak, B. Tomaszewska, A. Machocki, W. Grzegorczyk and A. Denis, Conversion of ethanol over supported cobalt oxide catalysts, *Catal. Today*, 2011, **176**(1), 14–20, DOI: 10.1016/j.cattod.2011.06.015.

21 H. Song, L. Zhang and U. S. Ozkan, Investigation of the Reaction Network in Ethanol Steam Reforming over Supported Cobalt Catalysts, *Ind. Eng. Chem. Res.*, 2010, **49**(19), 8984–8989, DOI: 10.1021/ie100006z.

22 E. Varga, K. Baan, G. F. Samu, A. Erdohelyi, A. Oszko, Z. Konya and J. Kiss, The Effect of Rh on the Interaction of Co with Al_2O_3 and CeO_2 Supports, *Catal. Lett.*, 2016, **146**(9), 1800–1807, DOI: 10.1007/s10562-016-1809-3.

23 S. Ogo, T. Shimizu, Y. Nakazawa, K. Mukawa, D. Mukai and Y. Sekine, Steam reforming of ethanol over K promoted Co catalyst, *Appl. Catal., A*, 2015, **495**, 30–38, DOI: 10.1016/j.apcata.2015.01.018.

24 A. Machocki, T. Ioannides, E. Papadopoulou and B. Banach, Hydrogen-rich gas generation from alcohols over cobalt-based catalysts for fuel cell feeding, *Fuel Process. Technol.*, 2016, **148**, 341–349, DOI: 10.1016/j.fuproc.2016.03.015.

25 S. J. Han, J. H. Song, J. Yoo, S. Park, K. H. Kang and I. K. Song, Sorption-enhanced hydrogen production by steam reforming of ethanol over mesoporous Co/CaO-Al_2O_3 xerogel catalysts: Effect of Ca/Al molar ratio, *Int. J. Hydrogen Energy*, 2017, **42**(9), 5886–5898, DOI: 10.1016/j.ijhydene.2016.12.075.

26 A. D. Shejale and G. D. Yadav, Cu promoted Ni-Co/hydrotalcite catalyst for improved hydrogen production in comparison with several modified Ni-based catalysts via steam reforming of ethanol, *Int. J. Hydrogen Energy*, 2017, **42**(16), 11321–11332, DOI: 10.1016/j.ijhydene.2017.03.052.

27 T. A. Maia, J. M. Assaf and E. M. Assaf, Study of Co/CeO_2-γ-Al_2O_3 catalysts for steam and oxidative reforming of ethanol for hydrogen production, *Fuel Process. Technol.*, 2014, **128**, 134–145, DOI: 10.1016/j.fuproc.2014.07.009.

28 S. A. Ghungrud and P. D. Vaidya, Improved Hydrogen Production from Sorption-Enhanced Steam Reforming of Ethanol (SESRE) Using Multifunctional Materials of Cobalt Catalyst and Mg-, Ce-, and Zr-Modified CaO Sorbents, *Ind. Eng. Chem. Res.*, 2020, **59**(2), 693–703, DOI: 10.1021/acs.iecr.9b05472.

29 Y. Xu, B. Lu, C. Luo, J. Chen, Z. Zhang and L. Zhang, Sorption enhanced steam reforming of ethanol over Ni-based catalyst coupling with high-performance CaO pellets, *Chem. Eng. J.*, 2021, **406**, 126903.

30 A. Iulianelli, V. Palma, G. Bagnato, C. Ruocco, Y. Huang, N. T. Veziroglu and A. Basile, From bioethanol exploitation to high grade hydrogen generation: Steam reforming promoted by a Co-Pt catalyst in a Pd-based membrane reactor, *Renewable Energy*, 2018, **119**, 834–843, DOI: 10.1016/j.renene.2017.10.050.

31 A. Casanovas, N. J. Divins, A. Rejas, R. Bosch and J. Llorca, Finding a suitable catalyst for on-board ethanol reforming using exhaust heat from an internal combustion engine, *Int. J. Hydrogen Energy*, 2017, **42**(19), 13681–13690, DOI: 10.1016/j.ijhydene.2016.11.197.

32 E. Moretti, L. Storaro, A. Talon, S. Chitsazan, G. Garbarino, G. Busca and E. Finocchio, Ceria-zirconia based catalysts for ethanol steam reforming, *Fuel*, 2015, **153**, 166–175, DOI: 10.1016/j.fuel.2015.02.077.

33 J. Y. Z. Chiou, C. L. Lai, S.-W. Yu, H.-H. Huang, C.-L. Chuang and C.-B. Wang, Effect of Co, Fe and Rh addition on coke deposition over $Ni/Ce_{0.5}Zr_{0.5}O_2$ catalysts for steam reforming of ethanol, *Int. J. Hydrogen Energy*, 2014, **39**(35), 20689–20699, DOI: 10.1016/j.ijhydene.2014.07.141.

34 W. Cai, N. Homs and P. R. de la Piscina, Renewable hydrogen production from oxidative steam reforming of bio-butanol over $CoIr/CeZrO_2$ catalysts: Relationship between catalytic behaviour and catalyst structure, *Appl. Catal., B*, 2014, **150–151**, 47–56, DOI: 10.1016/j.apcatb.2013.11.032.

35 W. Cai, P. R. de la Piscina, K. Gabrowska and N. Homs, Hydrogen production from oxidative steam reforming of bio-butanol over CoIr-based catalysts: Effect of the support, *Bioresour. Technol.*, 2013, **128**, 467–471, DOI: 10.1016/j.biortech.2012.10.125.

36 S. S.-Y. Lin, D.-H. Kim, M. H. Engelhard and S.-Y. Ha, Water-induced formation of cobalt oxides over supported cobalt/ceria-zirconia catalysts under ethanol-steam conditions, *J. Catal.*, 2010, **273**(2), 229–235, DOI: 10.1016/j.jcat.2010.05.016.

37 E. B. Pereira, P. R. de la Piscina, S. Marti and N. Homs, H_2 production by oxidative steam reforming of ethanol over K promoted $Co\text{-}Rh/CeO_2\text{-}ZrO_2$ catalysts, *Energy Environ. Sci.*, 2010, **3**(4), 487–493, DOI: 10.1039/b924624j.

38 S. S.-Y. Lin, H. Daimon and S. Y. Ha, $Co/CeO_2\text{-}ZrO_2$ catalysts prepared by impregnation and coprecipitation for ethanol steam reforming, *Appl. Catal., A*, 2009, **366**(2), 252–261, DOI: 10.1016/j.apcata.2009.07.010.

39 S. S.-Y. Lin, D. H. Kim and S. Y. Ha, Hydrogen Production from Ethanol Steam Reforming Over Supported Cobalt Catalysts, *Catal. Lett.*, 2008, **122**(3–4), 295–301, DOI: 10.1007/s10562-007-9375-3.

40 H. Song and U. S. Ozkan, Ethanol steam reforming over Co-based catalysts: Role of oxygen mobility, *J. Catal.*, 2009, **261**(1), 66–74, DOI: 10.1016/j.jcat.2008.11.006.

41 A. Machocki, A. Denis, W. Grzegorczyk and W. Gac, Nano- and micro-powder of zirconia and ceria-supported cobalt catalysts for the steam reforming of bio-ethanol, *Appl. Surf. Sci.*, 2010, **256**(17), 5551–5558, DOI: 10.1016/j.apsusc.2009.12.137.

42 A. Ishihara, Y. Maejima, H. Nasu and T. Hashimoto, Hydrogenation of carbon monoxide in the presence of solvent using novel carbon-oxide composite supported cobalt and iron catalysts, *J. Jpn. Pet. Inst.*, 2018, **61**, 51–58.

43 A. Ishihara, H. Aoki, T. Hashimoto and H. Nasu, Hydrothermal Gasification of Phenol Water on Novel Carbon-Supported Ni Catalysts Prepared by the Sol-Gel Method Using PEG, *J. Jpn. Inst. Energy*, 2013, **92**(8), 687–694.

44 A. Ishihara, T. Imai, T. Hashimoto and H. Nasu, Hydrothermal gasification of phenol water on novel carbon-supported Ni catalysts prepared by the sol–gel method using tartaric acid and alminum tri-sec-butoxide, *Fuel Process. Technol.*, 2015, **136**, 34–40.

45 A. Ishihara, K. Imanishi, T. Hashimoto and H. Nasu, Effects of types of metal oxides on hydrothermal gasification of phenol over novel metal oxide-carbon composite supported Ni catalysts prepared by sol-gel method, *J. Jpn. Pet. Inst.*, 2015, **58**, 302–311.

46 A. Teramachi, K. Yamashita and T. Yamamoto, Effects of Metal Ion Addition on the Crystalline Phase of Zirconium Dioxide Studied by X-Ray Diffraction Spectrometry, *Adv. X-Ray Chem. Anal., Jpn.*, 2013, **44**, 269–277.

47 P. Biswas and D. Kunzru, Steam reforming of ethanol on Ni-CeO2-ZrO2 catalysts: Effect of doping with copper, cobalt and calcium, *Catal. Lett.*, 2007, **118**(1–2), 36–49, DOI: 10.1007/s10562-007-9133-6.

48 A. R. Passos, L. Martins, S. H. Pulcinelli, C. V. Santilli and V. Briois, Correlation of Sol-Gel Alumina-Supported Cobalt Catalyst Processing to Cobalt Speciation, Ethanol Steam Reforming Activity, and Stability, *ChemCatChem*, 2017, **9**(20), 3918–3929, DOI: 10.1002/cctc.201700319.

49 Z. Ferencz, E. Varga, R. Puskas, Z. Konya, K. Baan, A. Oszko and A. Erdohelyi, Reforming of ethanol on Co/Al_2O_3 catalysts reduced at different temperatures, *J. Catal.*, 2018, **358**, 118–130, DOI: 10.1016/j.jcat.2017.12.003.

50 E. Martono and J. M. Vohs, Support effects in cobalt-based ethanol steam reforming catalysts: Reaction of ethanol on Co/CeO_2/YSZ(1 0 0) model catalysts, *J. Catal.*, 2012, **291**, 79–86, DOI: 10.1016/j.jcat.2012.04.010.

51 H. Song, X. Bao, C. M. Hadad and U. S. Ozkan, Adsorption/Desorption Behavior of Ethanol Steam Reforming Reactants and Intermediates over Supported Cobalt Catalysts, *Catal. Lett.*, 2011, **141**(1), 43–54, DOI: 10.1007/s10562-010-0476-z.

52 J. Sun, A. M. Karim, D. Mei, M. Engelhard, X. Bao and Y. Wang, "New insights into reaction mechanisms of ethanol steam reforming on $Co-ZrO_2$", *Appl. Catal., B*, 2015, **162**, 141–148.